Available online at www.sciencedirect.com

ScienceDirect

Procedia Environmental Sciences 2 (2010) 1881–1893

Procedia Environmental Sciences

International Society for Environmental Information Sciences 2010 Annual Conference (ISEIS)

# Bridge Afflux Predictions Using the Lattice Boltzmann Method

H. Liu[a,b,*], M. Li[a], J. G. Zhou[b], R. Burrows[b]

[a] *State Key Laboratory of Water Environment Simulation.*
*The Key Laboratory of Water and Sediment Sciences, Ministry of Education, China.*
*School of Environment, Beijing Normal Universitl, 19 Xinjiekou Wai Street，Beijing 100875, PR China.*
[b] *Department of Engineering, University of Liverpool, Brownlow Hill, Liverpool L69 3GQ, U.K.*

**Abstract**

The maximum water surface change just upstream of a bridge is termed the afflux in hydraulic engineering. An initial attempt at using the lattice Boltzmann method (LBM) to study afflux has been made in this paper. The LBM representing the 2D nonlinear shallow water equations (LABSWE) is applied to both single-span and multi-span bridges with a free water surface without introducing additional empirical coefficients. For a single-span bridge, three configuration parameters, blockage ratio, skewness and eccentricity, are investigated by the LBM; for a multi-span bridge, the influence of pier shape and skewness on afflux is also tested. The results agree closely with those of traditional methods, which illustrates that LABSWE is not only able to compute average afflux but also to show the afflux distribution across the section and the flow distribution around the obstruction.



Keywords:Bridge afflux; LABSWE; lattice Boltzmann method; nonlinear shallow water equations; blockage ratio; skewness; eccentricity.

## 1. Introduction

Afflux is defined as the increase in upstream water depth as a result of constriction of a flow channel. Prior to the placement of a bridge across a watercourse, the water surface for a given flood discharge may be assumed a normal profile. Due to the constriction imposed by the presence of the structure, the water level at a location upstream of it will increase (see Fig. 1). Bridge afflux is one of the key concerns in the design of a bridge construction. The UK Environment Agency requires no increase in flooding risk after construction of a new bridge. However, it is not easy to precisely assess afflux since it can be influenced by many factors. After examining the flow through different bridge piers experimentally, Yarnell generated an empirical equation showing that afflux is a function of downstream Froude number and the ratio of velocity head to depth at the upstream cross section [1]. In 1978, Bradley related the amount of afflux to channel Froude number and contraction ratio [2], which is also known as the USBPR (US Bureau of Public Roads) method. The HRC (H.R. Wallingford Arch) method developed in 1988, based on scale model study and field data, relates the ratio of afflux to downstream depth, downstream Froude

* Corresponding author. Tel./Fax: +86-10-58801719.
*E-mail address*: Haifei.liu@liv.ac.uk.

1878-0296 © 2010 Published by Elsevier Open access under CC BY-NC-ND license.
doi:10.1016/j.proenv.2010.10.200

number and blockage ratios [3,4]. Kaatz et al. in 1997 tested the accuracy of four 1D methods with measured field data [5]. In 2000, Ghodsian et al. carried out the experiments to test the effects of different parameters on the amount of afflux due to rectangular bridge piers [6]. In 2005, Seckin and Atabay experimentally analyzed the afflux around bridge waterways [7]. In addition, the recent research on afflux carried out by the UK Environment Agency also lists other factors such as roughness, the ratio of length to breadth, etc [8]. Regarding these factors, traditional 1D methods generally involve corresponding coefficients in governing equations like contraction and expansion coefficients in energy methods, drag coefficient in momentum methods etc, which inevitably introduces inaccuracy into afflux computation. With development of computing power, traditional 2D methods, which are well accepted such as finite difference, finite element and finite volume methods, are more frequently used in engineering than before, although 1D models still prevail. It is difficult and inconvenient, however, to apply different boundary conditions using these traditional 2D methods, especially for the flow-structure interaction problems where the complex boundaries play an important role. In recent decades, the lattice Boltzmann method (LBM) developed into an alternative method for simulating surface water flow. In the early 1990s, the Navier-Stokes equations were recovered by the LBM with the Bhatnagar-Gross-Krook (BGK) model [9,10]. Since 1999, several researchers proposed improved theories on the LBM for nonlinear shallow water equations [11,12], which introduced the LBM into river and coastal engineering. From the view of practical engineering, however, the applicability and validity are still not clear. As a result, engineers may not be confident to solve complex problems using the LBM.

In this paper, an original attempt has been made to analyze the bridge afflux with the relatively new tool, the lattice Boltzmann method. The objectives are to investigate the performance of 2D LBM in terms of bridge afflux computation by comparing its results with traditional methods, and to assess the influences of different aspects of the bridge configuration using the LBM. Since only the influence of the bridge is under consideration, the influences of wind stress and bed shear stress are not involved. Usually a bridge design must satisfy that the water surface of a particular flood event, such as 50-year or 100-year event, flows consistently below the soffit of bridge. So only bridges with free-surface subcritical flow are studied in this paper, and the flows of extreme flood events with water surface higher than the soffit of the bridge or even causing weir flow across the deck are not included.

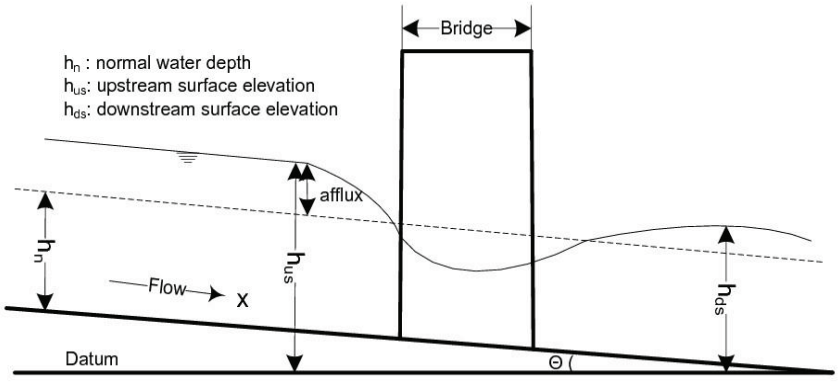


Fig. 1. Afflux Sketch

## 2. Governing Equations and Computational Method

### *2.1. Nonlinear Shallow Water Equations*

Shallow water flow is one of the most frequent situations in nature, representing flows in rivers, channels, coastal areas, estuaries and harbors. In this situation, water depth is usually much smaller than horizontal scale so that flow is characterized by near horizontal motion. The assumption of hydrostatic pressure is often then used to replace the momentum equation in the vertical direction in the mathematical model, so the vertical acceleration is ignored. The

general 2D governing equations for shallow water flows can be derived from the Navier-Stokes equations. After making depth-averaged calculations, the nonlinear shallow water equations can be written in a tensor form as [13]:

$$\frac{\partial h}{\partial t}+\frac{\partial\left(hu_j\right)}{\partial x_j}=0 \tag{1}$$

$$\frac{\partial\left(hu_i\right)}{\partial t}+\frac{\partial\left(hu_iu_j\right)}{\partial x_j}=-\frac{g}{2}\frac{\partial h^2}{\partial x_i}+\nu\frac{\partial^2\left(hu_i\right)}{\partial x_j\partial x_j}+F_i \tag{2}$$

where $h$ is water depth; $x_j$and $u_j$ are the distance and velocity components in the $j$ direction respectively, i.e. for $j= 1$, $x_j = x$ and $u_j = u$; for $j = 2$, $x_j = y$ and $u_j = v$. $x$ and $y$ are defined as longitudinal and lateral directions of the channel; $g = 9.81\ m/s^2$ is gravitational acceleration; $t$ is time; $\nu$ is kinetic viscosity; $F_i$ is the force term and is defined as:

$$F_i=-gh\frac{\partial z_b}{\partial x_i}+\frac{\tau_{wi}}{\rho}-\frac{\tau_{bi}}{\rho} \tag{3}$$

where $z_b$ is bed elevation above datum. The bed shear stress $\tau_{bi}$ in the $i$ direction is given by the depth-averaged velocities, $\tau_{bi}=\rho C_b u_i\sqrt{u_ju_j}$ , in which $C_b$ is the bed friction coefficient estimated from $C_b = g/C_z^2$, $C_z$ is the Chezy coefficient, either given by Manning equation, $C_z=h^{1/6}/n_b$, where $n_b$ is the Manning's coefficient, or the Colebrook-White equation [14],

$$C_z=-\sqrt{32g}\lg\left(\frac{K_s}{14.8h}+\frac{1.255\nu C_z}{4h\sqrt{2gu_ju_j}}\right) \tag{4}$$

where $K_s$ is the Nikuradse equivalent sand roughness. The wind shear stress $\tau_{wi}=\rho_a C_w u_{wi}\sqrt{u_{wj}u_{wj}}$ , where $\rho_a$ is the density of air, $C_w$ is the resistance coefficient, and $u_{wi}$ is the component of the wind velocity in the $i$ direction.

### *2.2. Lattice Boltzmann Method*

The lattice Boltzmann method is a discrete computational method based upon lattice gas cellular automata. A lattice Boltzmann model has three main components: the kinetic equation; lattice pattern and the equilibrium distributions. The lattice Boltzmann model for nonlinear shallow water equations (LABSWE) has been presented by Zhou [15], in which the lattice Boltzmann equation with 9-speed square lattice and force term is

$$f_\alpha\left(x+e_\alpha\Delta t,t+\Delta t\right)=f_\alpha\left(x,t\right)-\frac{1}{\tau}\left[\left(f_\alpha\left(x,t\right)-f_\alpha^{eq}\left(x,t\right)\right)\right]+\frac{\Delta t}{6e^2}e_{\alpha i}F_i \tag{5}$$

where $f_\alpha$ is the particle distribution function; $e = \Delta x/\Delta t$; $\Delta x$ is the square lattice size; $\Delta t$ is the time step; $\tau$ is dimensionless single relaxation time; $F_i$ is the force component in the $i$ direction; $e_{\alpha i}$ is the velocity vector of a particle in the $\alpha$ link. For the 9-speed square lattice shown in Fig. 2, each particle moves one lattice unit at its velocity along one of the eight links indicated with number 1-8, or else 0 indicates the particle at rest with zero speed. The velocity vector of particles is defined by

$$e_\alpha = \begin{cases} (0,0), & \alpha = 0 \\ e\left[\cos\dfrac{(\alpha-1)\pi}{4}, \sin\dfrac{(\alpha-1)\pi}{4}\right], & \alpha = 1,3,5,7 \\ \sqrt{2}e\left[\cos\dfrac{(\alpha-1)\pi}{4}, \sin\dfrac{(\alpha-1)\pi}{4}\right], & \alpha = 2,4,6,8 \end{cases} \tag{6}$$

The local equilibrium distribution function is expressed as [11,13].

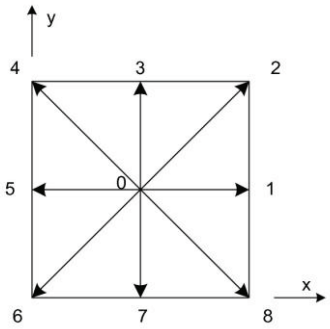


Fig. 2. D2Q9

$$f_\alpha^{eq} = \begin{cases} h - \dfrac{5gh^2}{6e^2} - \dfrac{2h}{3e^2}u_i u_i, & \alpha = 0 \\ \dfrac{gh^2}{6e^2} + \dfrac{h}{3e^2}e_{\alpha i}u_i + \dfrac{h}{2e^4}e_{\alpha i}e_{\alpha j}u_i u_j - \dfrac{h}{6e^2}u_i u_i, & \alpha = 1,3,5,7 \\ \dfrac{gh^2}{24e^2} + \dfrac{h}{12e^2}e_{\alpha i}u_i + \dfrac{h}{8e^4}e_{\alpha i}e_{\alpha j}u_i u_j - \dfrac{h}{24e^2}u_i u_i, & \alpha = 2,4,6,8 \end{cases} \tag{7}$$

From the distribution function, the physical variables water depth $h$ and flow velocity $u_i$ can be calculated:

$$h = \sum_\alpha f_\alpha, \quad u_i = \frac{1}{h}\sum_\alpha e_{\alpha i} f_\alpha \tag{8}$$

The actual dynamics of fluid flow is highly dependent on the surrounding environment. Boundary conditions play a crucial role since they select solutions which are compatible with external constraints [16]. The lattice Boltzmann equation can be solved with proper boundary conditions, such as the bounce-back scheme of no-slip

boundary conditions for highly rough boundaries, the elastic-collision scheme of slip or semi-slip boundary conditions for slide or medium rough boundaries [12], etc. At the inflow and outflow boundaries, as applied here, zero gradient of the distribution function normal to the boundary is often satisfactory. Also, the discharge at the inflow boundary is kept constant for each single afflux calculation consistent with the steady state conditions under consideration.

## 3. Bridge Model Tests

To validate the lattice Boltzmann model (LBM) in bridge afflux assessment, the LBM is applied here for two cases: single-span and multi-span bridges. For the single-span bridge, three configuration parameters are investigated: blockage ratio, skewness and eccentricity. For the multi-span bridge, two parameters are tested: pier shape and skewness. Blockage ratio, as one of the key influencing factors for bridge afflux, is defined as the ratio of blockage area to the whole area of the structure in front elevation; Skewness is defined as the angle between the normal to the flow direction and the bridge axis (see Fig.3(a)). Generally the skewness is smaller than 45 degrees; Eccentricity is defined as the value calculated by subtracting the ratio of the smaller abutment length to the larger abutment length across the flow area from one (see Fig.3(b) and Eq.(9)). To indicate maximum eccentricity when the bridge opening is flush with one of the channel sides, this ratio is subtracted from unity. The eccentricity range is therefore from zero (for which abutment lengths are equal) to unity (for which one abutment length is zero).

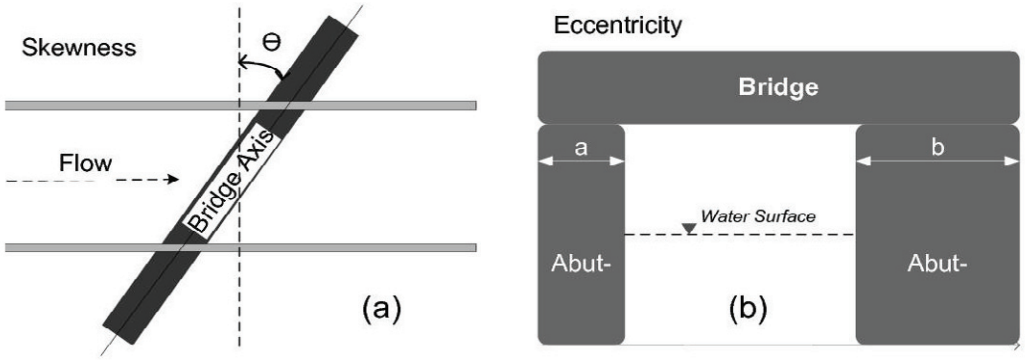


Fig. 3. (a) Skewness; (b) Eccentricity

$$E = \begin{cases} 1 - b/a, & for \quad b < a \\ 1 - a/b, & for \quad a < b \end{cases} \quad (E \text{ is eccentricity.}) \tag{9}$$

The most popular 1D methods for computing afflux, the HRC-USBPR method (used in the ISIS Package [17]) and the energy method (used in the HEC-RAS Package [18]), are applied for comparison of the LBM. Being based on conservation of energy or momentum across the bridge structure, these methods obtain the average afflux by involving empirical coefficients to model contraction, expansion or drag phenomena, which will inevitably be imprecise. Consequently, one of the well-accepted finite volume methods (FVM), SIMPLEC method within the Fluent Software [19], has also been used for verification of the LBM lateral afflux distributions.

### *3.1. Afflux of a Single-Span Bridge*

#### *3.1.1. Model Setup*

For the single-span bridge, a beam bridge model is selected within the dimensions of Seckin and Atabay's experimental models [7]. A beam bridge with two *20cm*×*20cm* (*length* × *width*) square abutments is added to a *1m*

wide channel. The bed slope is *0.02*; the Manning *n* is set to *0.070*; the velocity is initialized to zero, and the downstream water depth, *h*, is a constant of *0.8m*; $\tau$ is *1.0*; a no-slip boundary condition is applied. The computational domain is *2m×1m* (*length × width*) with *200×102* grids. The inflow is kept constant for each single afflux calculation. The flow becomes steady when the iteration number of the computation is bigger than 5000 and a series of afflux results are obtained with the changes of discharge.

*3.1.2. Results and Parameter Study*

From previous research [7], the energy method generally produced more accurate results for all bridge models when compared with experimental data and the average errors are within *-3.2%* and *0.8%* in terms of flow depth, whereas the average errors of the HRC-USBPR method are from *-0.2%* to *5.2%*. Since the LBM applied in this study is a 2D model being able to calculate afflux at each node, comparison with the 2D FVM (SIMPLEC in Fluent 6.3.26 Software) result is carried out (see Fig. 4(a)) and the mean afflux of the analyzed cross section is used to compare with the other 1D data. Fig. 4(a) shows a good agreement between the LBM and SIMPLEC results with respect to the lateral afflux distribution; whilst Fig. 4(b) shows that the afflux curve obtained by the LBM is very close to that of energy method with an average *0.003m* difference, being *0.4%* in terms of water depth. Hence it is apparent that the LBM result is accurate enough for engineering purposes.

As part of the parameter study, the blockage ratio was varied from 40% to 80%, and the corresponding afflux calculated by the LBM is plotted in Fig. 5(a). It can be seen that the afflux increases with the ascending blockage ratios. If a 4th degree polynomial is used for data fitting, a good agreement can be obtained in Fig. 6. The effect of skewness, ranging from 0 degree to 45 degrees in this model, is also tested by the LBM. The results are plotted in Fig. 5(b), which indicate that the increase of skewness also causes increase of afflux. However, its contribution is far less than that of blockage ratio. Finally, different eccentricities coupled with four blockage ratios have been simulated. As shown in Fig. 7, there is little influence generated by the change of eccentricity for any blockage ratio. The reasons for this are that the scale of the model tested is too small to show the afflux change for different eccentricities and the geometry does not change along the channel.

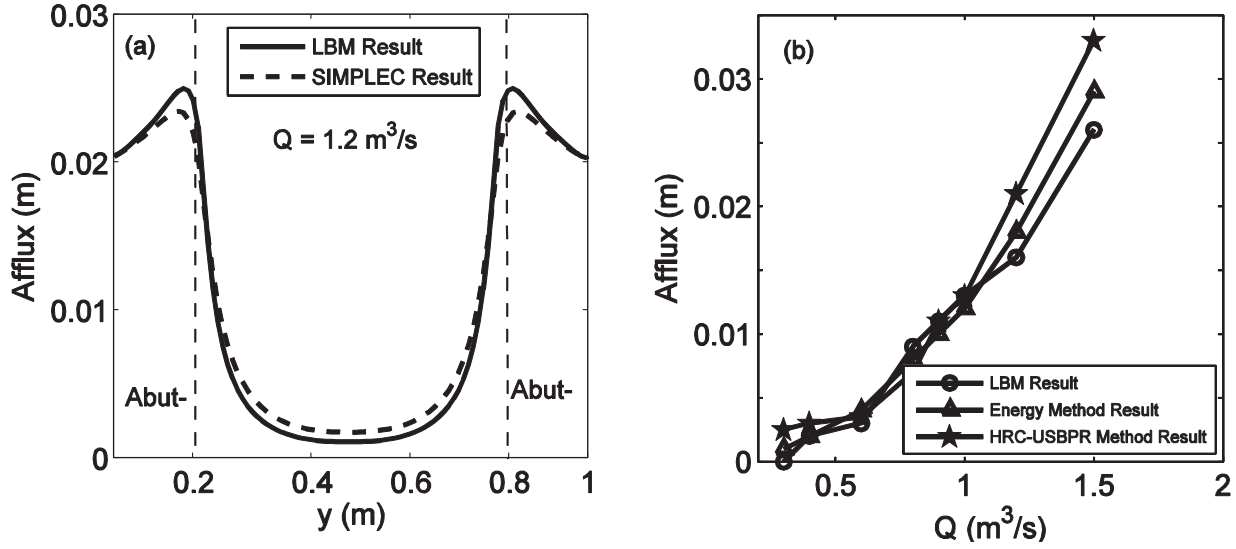


Fig. 4. (a) Afflux Distributions at 0.1m Upstream of the Single-Span Bridge; (b) Afflux Curves Comparison

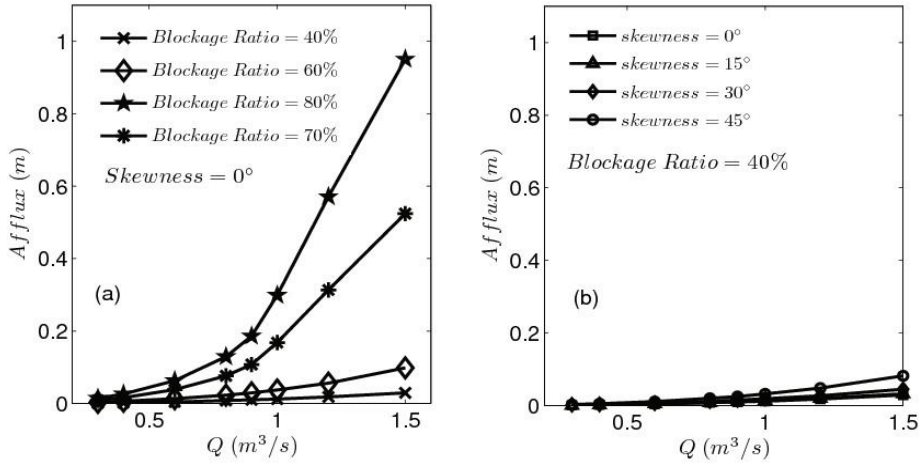


Fig. 5. Afflux Curves for the Single-Span Bridge with Different Blockage Ratios and Skewness

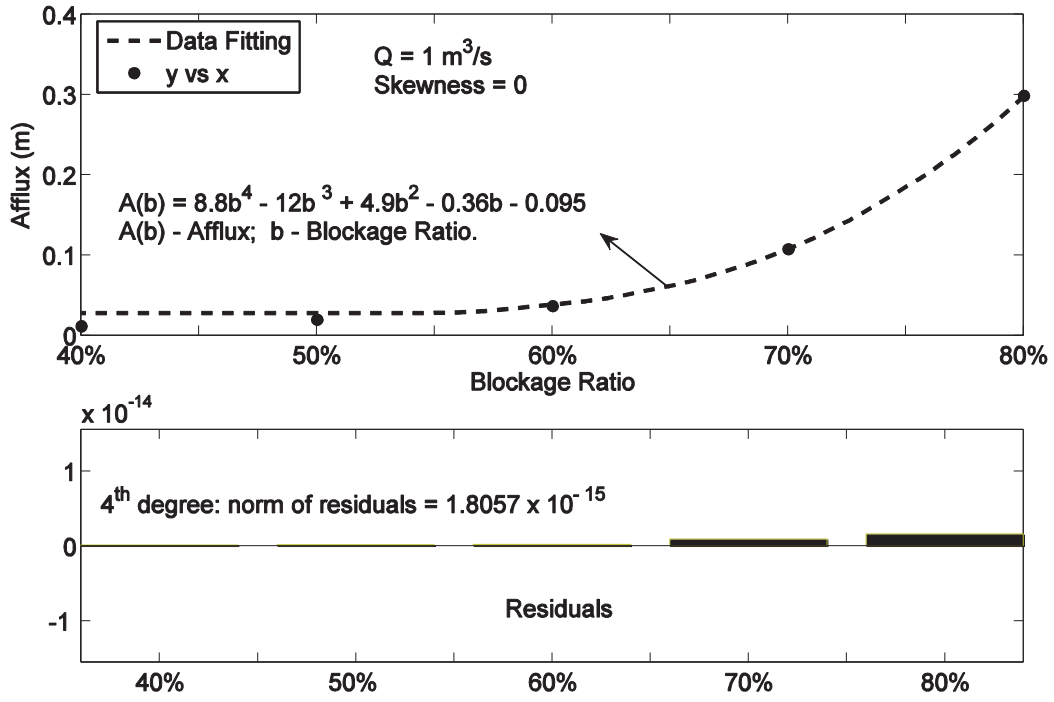


Fig. 6. Afflux-Blockage Ratio Relationship

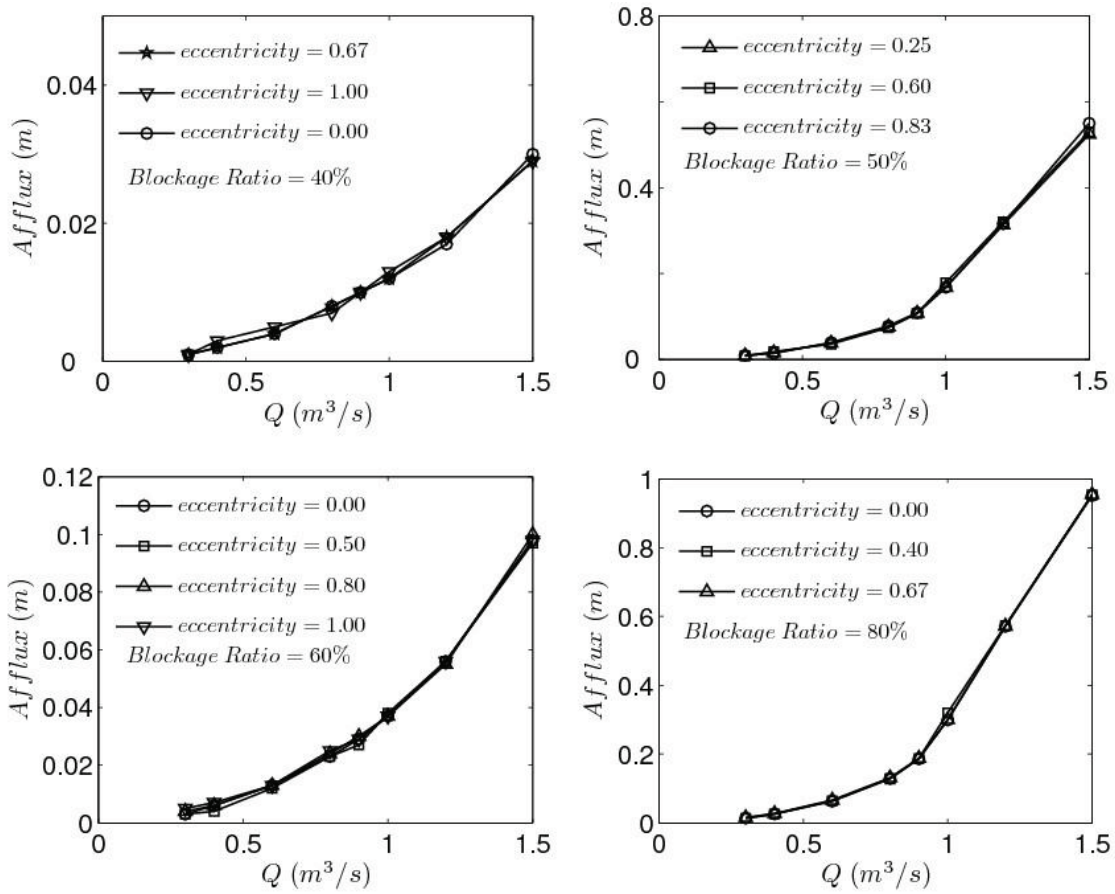


Fig. 7. Afflux Curves for the Single-Span Bridge with Different Eccentricities

### *3.2. Afflux of a Multi-Span Bridge*

#### *3.2.1. Model Setup*

For a more complex situation, the case of a multi-span bridge with two rectangular piers (see Fig. 8) is investigated. The bed slope is *0.02*; the Manning *n* is set to *0.070*; the velocity is initialized to zero, the downstream water depth, *h*, is a constant of *1.8m* and $\tau$ is 1.0; time step is *0.005s*; the no-slip boundary condition is applied; the computational domain is *40m*×*10m* (*length* × *width*) with a *400*×*102* grid. The inflow is kept constant for each single afflux calculation. The flow becomes steady when the iteration number of the computation is bigger than 27000 and a series of afflux results are obtained with change of discharge. Then two situations, the variations of pier shapes and the skewness for the multi-span bridge, are simulated. The LBM result are compared with that of the Yarnell equation [1] that is sensitive to the pier shapes.

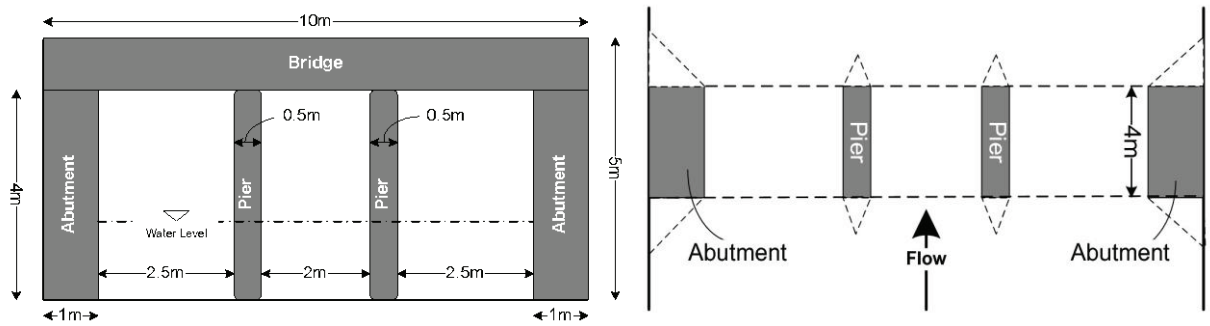


Fig. 8. Front Elevation and Plan View

*3.2.2. Results and Parameter Study*

The velocity histories of one particular point, representing the convergence speed, are plotted in Fig. 9. The coordinates of the point are (*10m, 5m*) in the center of the channel. In fact, such velocities are constants after the steady state is reached. The afflux curves (see Fig. 10(a)) show a good agreement with the Energy method indicating that the LBM is able to give excellent afflux estimation. After changing the rectangular abutments and piers to be those with triangular toes, the LBM result is slightly higher than that of the Yarnell equation with only *0.003m* maximum difference being *0.2%* in terms of water depth. Since the Yarnell equation generally computes afflux lower than the measured afflux due to the neglect of entrance friction [5], the LBM result is likely closer to reality.

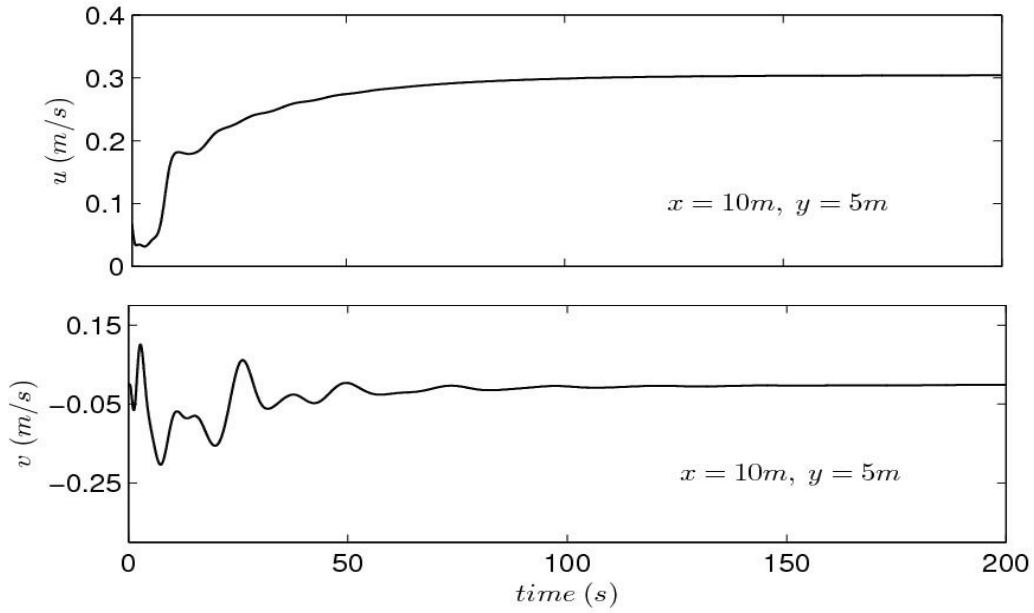


Fig. 9. Velocity Histories at a Particular Point ($Q=0.5m^3/s$)

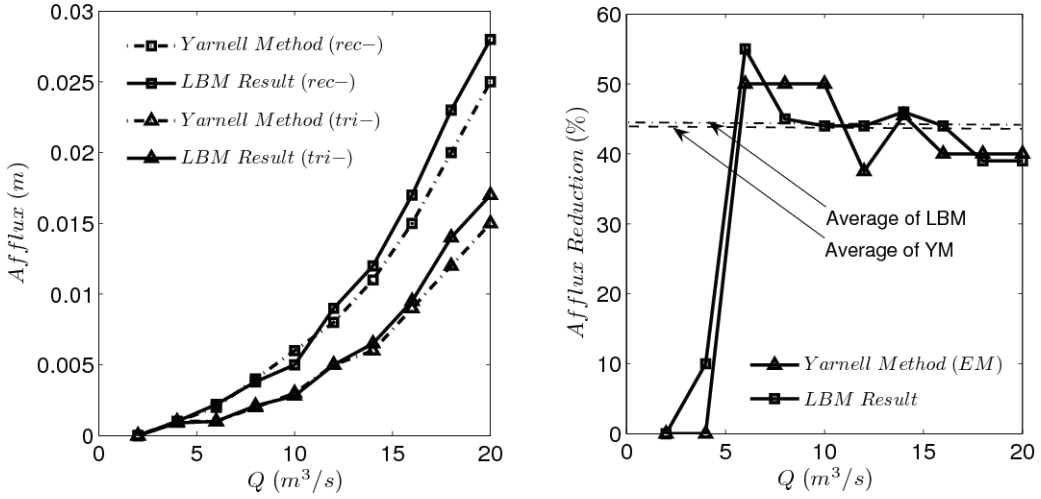


Fig. 10. (a) Afflux Curves; (b) Afflux Reduction

The variation of the shape of piers and abutments, here represented by changing from rectangular to triangular, causes a reduction of the afflux. From Fig. 10(b), except the first few low flows, both the LBM and the Yarnell results indicate that afflux is reduced by at least *40%* by the triangular piers and abutments of better streamline shape, which shows that the lattice Boltzmann model performs an accurate simulation of different pier shapes. Validation of the afflux distribution plots based on the LBM is again obtained by comparison against the FVM (SIMPLEC) results as shown in Fig. 11. The influence of skewness on afflux has also been assessed using the LBM. From Fig. 12(a), the larger skewness results in larger afflux although the absolute values are still small. Take *Q = 10*, *14* and *18m³/s* for examples (see Fig. 12(b)): the afflux increases exponentially with skewness, but afflux is lower than *0.08m*. Therefore the effect of skewness is seen to be minor compared with that of blockage ratio. The velocity field in conjunction with free surface elevation around the skewed bridge model obtained from the LBM is shown in Fig. 13.

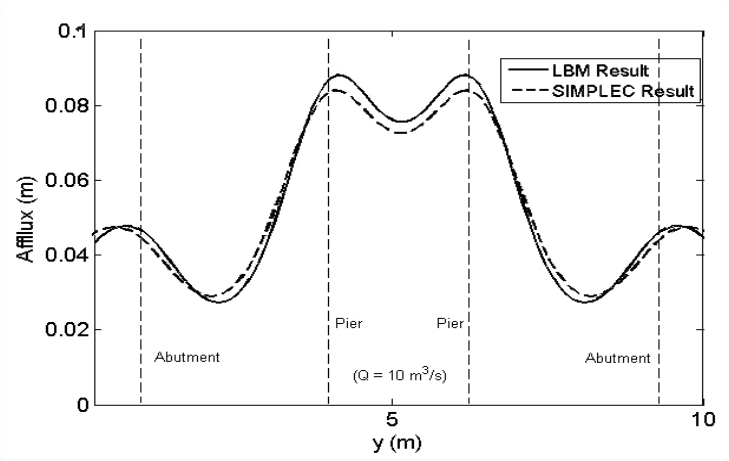


Fig. 11. Afflux Distributions at *0.5m* Upstream of the Multi-Span Bridge with Rectangular Piers (*Q=10 m³/s*)

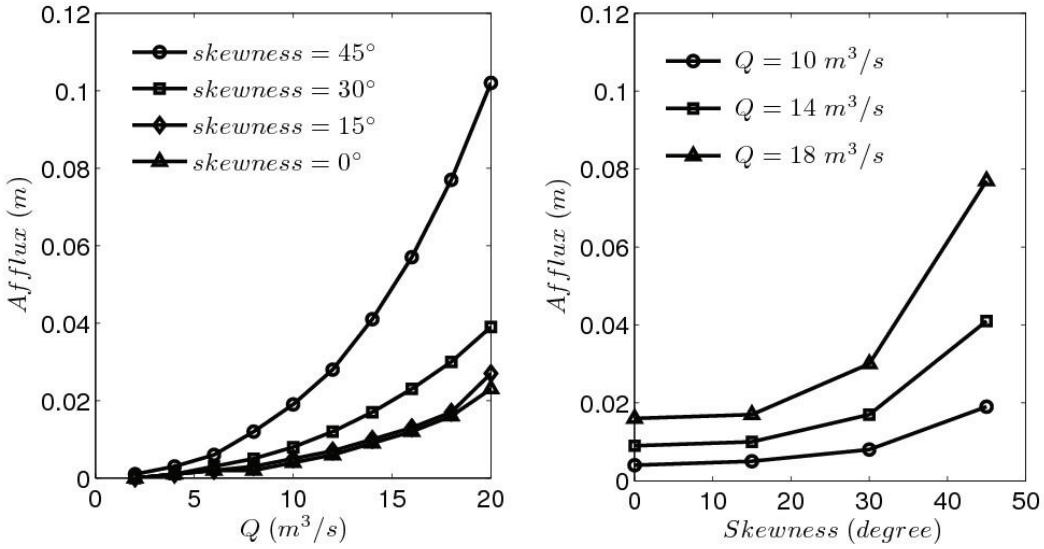


Fig. 12. LBM Afflux Curves for Multi-Span Bridge with Different Skewness

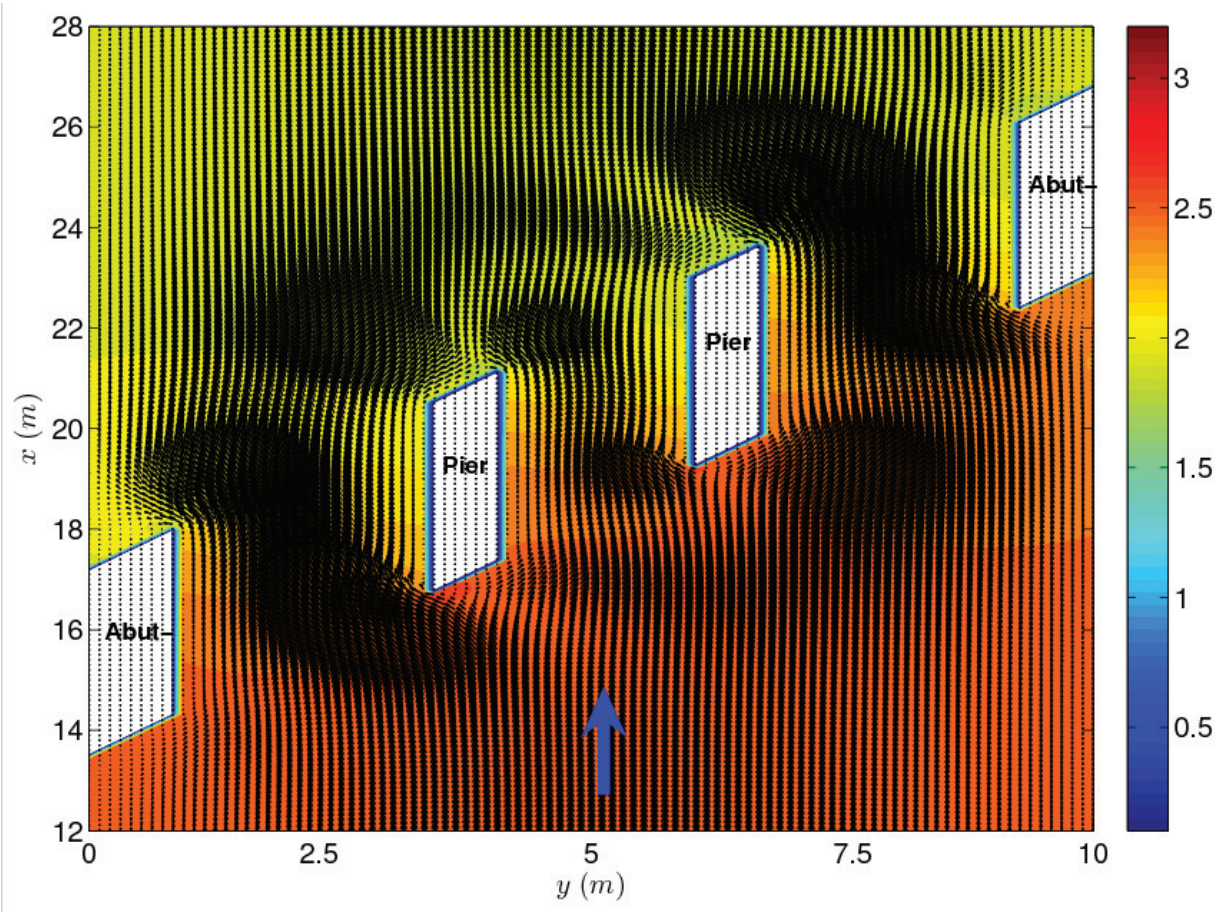


Fig. 13. Velocity Field and Surface Elevation for Skewed Multi-Span Bridge ( *Skewness=45 degrees*, *Q=10 m³/s*)

### *3.3. Results Summary and Discussion*

The relevant factors of afflux, blockage ratio, skewness, eccentricity and pier shape, have been tested by the lattice Boltzmann method. Based on the results shown earlier, blockage ratio is the key contributing factor for afflux; furthermore, the increase of afflux can be exponential either for single-span bridge or multi-span bridge. When the skewness is enlarged, the afflux correspondingly rises for both bridge types but the effect is not as significant as that of blockage ratio. For the single-span bridge tested in *Section 3.1*, the eccentricity has little influence on afflux due to the limit of model scale and the simple geometry; For the multi-span bridge investigated, the afflux caused by triangular piers is smaller than that caused by rectangular pier, by more than *40%*.

The LBM results have been compared with both 1D and 2D traditional methods. Good agreement has been achieved. Compared with the 1D methods, the LBM can provide detailed afflux distributions, although more computing effort is required. Compared with a standard 2D FVM computational approach, the flexibility of the LBM in applying the boundary conditions is more convenient and efficient, and this advantage may be more obvious when the bridge or geometry is complex. Furthermore, the computational time required by the same task for the LBM is relatively shorter than the FVM, being *36* and *45 hours* respectively for the multi-span bridge simulations in a DELL E520 machine. However, the LBM is only conditionally convergent so that more care must be taken when constructing the models. The detailed stability analysis of the LBM can be found in [20].

For extreme events when flow conditions such as pressure flow or weir flow happens when the water level exceeds the bridge soffit, there are more factors that can influence bridge afflux, such as the size and shape of the bridge deck. In order to analyze the detailed flow structure in this situation, 3D lattice Boltzmann modeling is needed. In addition, there will be a new challenge for the bridge afflux calculation at watercourses with steeper slope and lower roughness values where supercritical flow takes place.

## 4. Conclusions

It is difficult to evaluate different methods for computing bridge afflux due to the lack of experimental or field data for testing, so further addition to the data base would be of considerable benefit. Successfully applying the LBM to the nonlinear shallow water equations makes the model suitable in many practical engineering problems involving open channel flows, tidal flows, waves etc. In this study, afflux for single-span and multi-span bridges in open channels of different configurations have been numerically simulated by the lattice Boltzmann model for the first time. The results have been compared with those obtained from traditional methods, indicating that the LBM is not only able to calculate average afflux, but also predict detailed afflux and flow distributions in the vicinity of the channel constriction. This provides a new means for accurate estimation of afflux, especially for complex bridge types.

## 5. Acknowledgement

The financial supports by The State Key Laboratory of Water Environment Simulation, National Natural Science Foundation of China (51009007), National Natural Science Foundation Grant for Distinguished Young Scholars (50625926) and National Basic Research Program of China (973) (2006CB403303, 2011CB403304) are gratefully acknowledged.

## References

[1] D. L. Yarnell. Pile trestles as channel obstructions. Technical Bulletin 429, U.S. Department of agriculture, Washington; 1934a.

[2] J. N. Bradley. Hydraulics of Bridge Waterways: Hydraulic Design. 2nd Edition. Federal Highway Administration, Washington, D.C.; 1978.

[3] P. M. Brown. Afflux at arch bridges, Report SR 182. HR Wallingford, UK; 1988.

[4] JBA Consulting. Afflux Advisor User Guide. Defra and Environment Agency; 2005.

[5] K. J. Kaatz, W. P. James. Analysis of alternatives for computing backwater at bridges. Journal of Hydraulic Engineering, Vol.123 No.9; 1997.

[6] M. Shafieefar, M. Ghodsian, SJ. Hashemi. Afflux due to rectangular bridge pier. ASCE Proceedings of Joint Conference on Water Resource Engineering, Planning and Management; 2000.

[7] Galip Seckin, Serter Atabay. Experimental backwater analysis around bridge waterways. Canadian Journal of Civil Engineering 32(6): 1015-1029; 2005.

[8] JBA Consulting. Research and Development Technical Report: Afflux at bridge and culverts. Defra/Environment Agency; 2005.

[9] S. Chen, H. Chen, WH. Matthaeus. Recovery of the Navier-Stokes equations using a lattice-gas Boltzmann method. Phys. Rev. A., 45: R5539-42; 1992.

[10] D. d'Humieres, YH. Qian, P Lallemand. Lattice BGK Models for Navier-Stokes equation. Europhys. Lett, 17: 479-84; 1992.

[11] R. Salmon. Lattice Boltzmann solutions of the three-dimensional planetary geostrophic equations. Journal of Marine Research, 57: 847–884; 1999.

[12] J. G. Zhou. An elastic-collision scheme for lattice Boltzmann methods. International Journal of Modern Physics C 12:387-401; 2001.

[13] J. G. Zhou. Lattice Boltzmann Methods for Shallow Water Flows, volume 1. Berlin, Germany; 2004.

[14] R. E. Featherstone, C.Nalluri. Civil Engineering Hydraulics. Hartnolls Ltd 3rd edition; 1995.

[15] J. G. Zhou. A lattice Boltzmann model for the shallow water equations with turbulence modeling. International Journal of Modern Physiscs C, Vol.13, No.8 1135-1150; 2002.

[16] Sauro Succi. The lattice Boltzmann equation for fluid dynamics and beyond. Oxford University Press; 2001.

[17] Halcrow/HR Wallingford. User's Manual of ISIS, Version 2.5. Halcrow Software and Wallingford Software Ltd; 2007.

[18] U.S. Army Corps of Engineers. User's Manual of HEC-RAS Version 3.1.3. Hydrologic Engrg. Ctr.; 2005.

[19] Fluent Europe Ltd. FLUENT 6 User’s Guide, volume 4. ANSYS/FLUENT Europe Ltd; 2001.

[20] J. D. Sterling, S. Chen. Stability analysis of Lattice Boltzmann Methods. Journal of Computational Physics, 123: 196-206; 1996.